Thermodynamic Analysis of Denaturant-Induced Unfolding of HodC69S Protein Supports a Three-State Mechanism

Kristian Boehm,[‡] Jessica Guddorf,[‡] Alexander Albers,[§] Tadashi Kamiyama,[||] Susanne Fetzner,[§] and H.-J. Hinz*[,‡]

Institut für Physikalische Chemie, Westfälische Wilhelms-Universität Münster, Corrensstrasse 30, 48149 Münster, Germany, Institut für Molekulare Mikrobiologie and Biotechnologie, Westfälische Wilhelms-Universität Münster, Corrensstrasse 3, 48149 Münster, Germany, and Department of Chemistry, Kinki University, 3-4-1 Kowakae, Higashi-Osaka, Osaka, Japan

Received March 31, 2008; Revised Manuscript Received May 7, 2008

ABSTRACT: Thermodynamic stability parameters and the equilibrium unfolding mechanism of His_6HodC69S, a mutant of 1*H*-3-hydroxy-4-oxoquinaldine 2,4-dioxygenase (Hod) having a Cys to Ser exchange at position 69 and an N-terminal hexahistidine tag (His_6HodC69S), have been derived from isothermal unfolding studies using guanidine hydrochloride (GdnHCl) or urea as denaturants. The conformational changes were monitored by following changes in circular dichroism (CD), fluorescence, and dynamic light scattering (DLS), and the resulting transition curves were analyzed on the basis of a sequential three-state model N = I = D. The structural changes have been correlated to catalytic activity, and the contribution to stability of the disulfide bond between residues C37 and C184 in the native protein has been established. A prominent result of the present study is the finding that, independent of the method used for denaturing the protein, the unfolding mechanism always comprises three states which can be characterized by, within error limits, identical sets of thermodynamic parameters. Apparent deviations from three-state unfolding can be rationalized by the inability of a spectroscopic probe to discriminate clearly between native, intermediate, and unfolded ensembles. This was the case for the CD-monitored urea unfolding curve.

1*H*-3-hydroxy-4-oxoquinaldine 2,4-dioxygenase (Hod), which catalyzes the oxygenolytic cleavage of its organic substrate to carbon monoxide and *N*-acetylanthranilate, is a catabolic enzyme involved in the pathway of quinaldine (2-methylquinoline) degradation by *Arthrobacter nitroguajacolicus* strain Rü61a. Remarkably, Hod is a cofactor-independent oxygenase belonging to the α/β-hydrolase fold family (*1, 2*). In a previous study (*3*), we reported thermal unfolding measurements of this protein. However, as wild-type Hod tends to form dimers due to oxidative formation of an intermolecular disulfide bridge, we have been using the protein with a C69S substitution for our biophysical and biochemical studies (*3, 4*). The catalytic properties of the enzyme are not affected by the C69S replacement and by an additional N-terminal hexahistidine tag.

The thermodynamic analysis of thermal unfolding of His_6HodC69S was based on differential scanning calorimetry (DSC),[1] circular dichroism (CD), differential scanning densimetry (DSD), and dynamic light scattering (DLS) data, all of which could be fitted globally to a three-state model involving a significantly populated intermediate. The thermodynamic parameters required for the calculation of the various fractions of native, intermediate, and unfolded states were obtained from the temperature dependence of the heat capacity curve as determined by DSC. This method provides by far the most accurate assessment of thermodynamic data of proteins at the transition temperature. However, in many cases knowledge of the stability of proteins at ambient temperature is required rather than at the high unfolding temperatures. Therefore, many stability parameters of proteins are not estimated from thermal unfolding studies but from isothermal GdnHCl or urea denaturation experiments to avoid possible errors introduced by an extrapolation of stability parameters over a temperature range of 30 or 40 °C. It has been observed by comparison of the results derived from the different approaches that often a notorious disagreement exists not only between the stability parameters derived from thermal and chemical unfolding studies but also between values obtained from GdnHCl and urea denaturation (*5–7*). This is disturbing, as in principle all methods of unfolding should provide the same thermodynamic parameters, if the different protein states have distinguishable properties and the data have been extrapolated properly to the same temperature and to identical buffer conditions (*5*). Despite the fundamental significance of the thermodynamic consistency only few studies were concerned with a systematic comparison of stability parameters and equilibrium unfolding mechanisms resulting from thermal and chemical unfolding procedures (*8–10*). None of these, to our knowledge, dealt with a fairly large protein, such as His_6HodC69S,

* To whom correspondence should be adressed. E-mail: hinz@uni-muenster.de. Telephone: 0049 251 8323427. Fax: 0049 251 8329163.

[‡] Institut für Physikalische Chemie, Westfälische Wilhelms-Universität Münster.

[§] Institut für Molekulare Mikrobiologie and Biotechnologie, Westfälische Wilhelms-Universität Münster.

[||] Department of Chemistry, Kinki University.

[1] Abbreviations: CD, circular dichroism; DLS, dynamic light scattering; DSC, differential scanning calorimetry; DSD, differential scanning densimetry; DTNB, 5,5′-dithiobis(2-nitrobenzoate); DTT, dithiothreitol; GdnHCl, guanidine hydrochloride.

10.1021/bi800554v CCC: $40.75
Published on Web 06/13/2008

showing three-state unfolding. We considered it therefore apposite to complement our thermal unfolding studies of His_6-HodC69S (*3*) by a detailed analysis of the isothermal denaturation by both GdnHCl and urea. Such an approach should shed some light on the fundamental question of the method-independent, universal validity of thermodynamic stability parameters of biological macromolecules. The denaturant-based isothermal transition curves were constructed from CD, fluorescence intensity, fluorescence λ_{max} shift, and dynamic light scattering data, and they were analyzed on the basis of the Gibbs energy parameters originally obtained from the previous DSC studies (*3*). As protein samples from different fresh preparations were used for the studies, we took care to check the validity of previous results by repeating some of the DSC and temperature-induced CD measurements.

It is a noticeable result of the present studies that the three-state unfolding mechanism of His_6HodC69S is a consistent feature of all unfolding processes, be they initiated by temperature increase or denaturant action. Only urea-induced, CD-monitored transitions appear to lack largely the three-state character indicated by other techniques.

MATERIALS AND METHODS

Protein Preparation and Characterization. His_6HodC69S was prepared and purified as described in detail by Beermann et al. (*3*) and Frerichs-Deeken et al. (*4*). The organic substrate of the enzyme, 1*H*-3-hydroxy-4-oxoquinaldine, was synthesized from 3-formyl-2-methyl-4(1*H*)-quinolone (*11*) as reported before (*12*). The catalytic activity of the protein was determined spectrophotometrically by measuring substrate consumption at 334 nm (*4*). One unit was defined as the amount of enzyme that converts 1 μmol of substrate per minute at 30 °C.

Protein concentration was measured at 280 nm with an X-Dap (1024) diode array spectrophotometer IKS (now axeon GmbH) using an extinction coefficient of 1.937 mL mg^{-1} cm^{-1}. The coefficient was calculated according the method of Pace et al. (*13*). Molar concentrations were calculated using a molar mass of 33240.4 g mol^{-1}.

Spectrophotometric Detection of Disulfide Bridges. To determine the number of free thiols or the occurrence of disulfide bridges in His_6HodC69S, we followed the modified Ellman (14) procedure published by Baker and Panow (15). It involves three steps: (1) addition of Ellman's reagent (DTNB) to native protein solution to obtain the number of solvent-accessible free cysteine residues, (2) unfolding the protein by urea (7 M) followed by DTNB addition to determine the number of buried cysteines, and (3) reducing the unfolded protein using $NaBH_4$ to determine the number of disulfide bridges. Reaction with DTNB was observed by the characteristic absorption at 412 nm of the DTNB anion. The number, N_{S-H}, of free thiol groups was calculated using the relation:

$$N_{S-H} = \frac{M_{protein} E_{412nm}}{\varepsilon_{DTNB,412nm} c_{protein} d} \quad (1)$$

$M_{protein}$ is the molar mass of the protein (g mol^{-1}), $\epsilon_{DTNB,412nm}$ = 12000 L mol^{-1} cm^{-1} is the molar extinction coefficient of DTNB at 412 nm (15), $c_{protein}$ is the protein concentration (g L^{-1}), and d is the path length of the cuvette (cm).

The protein concentration used in the cell was 0.26 mg mL^{-1} to produce absorption changes that guarantee highly accurate UV measurements.

Urea and GdnHCl Equilibrium Unfolding Measurements. Stock solutions **I** and **II** of native protein in 10 mM sodium phosphate and 10 mM sodium borate buffer, pH 7.5, contained 1 mg mL^{-1} or ~10 mg mL^{-1}, respectively. Denaturant stock solutions contained 8 M GdnHCl or 10 M urea in the same buffer. The protein stock solutions were employed to generate by dilution different denaturant concentrations with a fixed final protein concentration of (**I**) 0.05 mg mL^{-1} and (**II**) 0.5 and 1 mg mL^{-1}. Reference solutions were made from buffer solution and denaturant stock solution. In general, the protein samples were incubated at 25 °C for 24 h to reach equilibrium. The final experimental concentration of His_6HodC69S was different for the various techniques and is given in the description of the experimental methods and in the figure legends.

Concentrations of urea and GdnHCl solutions were determined from measurements of their refractive indices at 25 °C using a Zeiss refractometer. Urea and GdnHCl concentrations were determined according to Nozaki (*16*) and Warren and Gordon (*17*) from the relationships

$$[\text{urea}] = 117.66\Delta n + 29.753\Delta n^2 + 185.56\Delta n^3 \quad (2)$$

$$[\text{GdnHCl}] = 57.147\Delta n + 38.68\Delta n^2 - 91.6\Delta n^3 \quad (3)$$

where Δn is respectively the difference between the refractive index of the denaturant solution and the buffer solution.

CD Measurements. CD measurements were carried out using a Jobin-Yvon (Paris, France) model CD-6 spectropolarimeter equipped with a Peltier-thermostated cell holder, constructed by the technical workshop of the Institute of Physical Chemistry, WWU Münster. The Peltier temperature control unit permits a variation of heating rates between 0.01 and 2.5 K min^{-1}. The maximal cooling rate is 1.3 K min^{-1}. Constancy of temperature is controlled to a precision of ±0.1 K. Quartz cells with an optical path length of 0.01 and 0.05 cm were used for protein concentrations of 1 and 0.5 mg mL^{-1}, respectively. The mean residue ellipticity $[\Theta]_{MRE}$ was calculated using the equation

$$[\Theta]_{MRE} = \frac{\Theta \times 100 \times MRW}{cd} \left(\frac{\text{deg} \cdot \text{cm}^2}{\text{dmol}}\right) \quad (4)$$

where Θ is the experimental ellipticity (deg), MRW = 115.4 g mol^{-1} is the mean residue weight (33240.4 g mol^{-1}/288 residues), c is the specific concentration (mg mL^{-1}), and d is the optical path length of the cell (cm).

(A) CD Spectra. Determination of urea and GdnHCl unfolding was performed by measuring spectra of the protein samples in the wavelength range from 190 to 260 nm with an increment of 0.5 nm and an integration time of 2 s. To improve the signal-to-noise ratio of the spectra, five scans per sample were performed routinely. Each measurement was corrected for buffer and denaturant contributions before averaging of the spectra.

(B) CD Heating Scans of Native and Reduced Proteins. Heating scans of protein solutions with and without DTT were monitored in a temperature range from 10 to 70 °C employing a protein concentration of 1 mg mL^{-1}. The heating rate was 1 K min^{-1}, and data were collected every 0.5 K. To obtain complete reduction of the protein, we

incubated the samples for 2 h with 40 mM DTT prior to scanning. Reference scans were made with buffer solution containing 40 mM DTT.

After reference correction the thermal transition curves were normalized to the $[\Theta]_{MRE,222nm}$ values of the denatured state at maximum temperature.

Fluorescence Measurements. Fluorescence studies were performed using a Spex Fluoromax spectrofluorometer thermostated by a Haake F3 water bath. Fluorescence emission spectra were monitored from 300 to 400 nm using an excitation wavelength of 295 nm for the nine tryptophans of His_6HodC69S. Spectral data were registered every 0.5 nm, using a slit width of 3 mm and an integration time of 2 s. The protein concentration was 0.05 mg mL^{-1} for the urea/GdnHCl denaturation experiments; a cuvette of 1 cm light path was used. All sample spectra were corrected for the signals of the respective reference solutions.

All measurements were performed at 25 °C. Denaturant-induced transition curves were constructed on the basis of changes in the emission intensity at 350 nm or from shifts of the maximum wavelength (λ_{max}) of the emission spectrum.

Dynamic Light Scattering (DLS) Studies. Light scattering experiments were performed using a DynaPro molecular sizing instrument (Wyatt Technology) which employs an 825.7 nm semiconductor laser as light source. After passing the sample the scattered light is collected at a fixed angle of 90°. During experiments the temperature was held at 25 ± 0.1 °C via a Peltier unit. Data analysis was made using the Dynamics 6.7.6 software package provided by the company. The translational diffusion coefficient, D_t, of the sample particles is determined by measuring the fluctuations in the intensity of the scattered light with an autocorrelator. The hydrodynamic radius, r_H, of the particles was calculated using the Stokes−Einstein equation $D_t = (k_B T)/(6\pi\eta r_H)$, where k_B is the Boltzmann constant, T is the absolute temperature, and η is solution viscosity in centipoise (mPa s).

The samples were prepared as described above for equilibrium unfolding measurements. Final protein concentrations of 0.05 or 1 mg mL^{-1} were used in the DLS measurements. Prior to DLS measurements the samples were filtered through a 0.2 μm filter (Anodisc 13; Whatman). We measured 18 samples using 0−5 M GdnHCl. Each sample measurement consisted of 50 acquisitions including 10 reads/acquisition and an automatically adjustable laser power output to a detected intensity of 500000 counts s^{-1}.

The calculated autocorrelation function of each acquisition was then analyzed using the intensity-weighted regularization model provided in the Dynamics software package. The data from the acquisitions which did not exceed a limit of ~0.01 between both curves were averaged after checking if the resulting data are consistent with a monodisperse size distribution (polydispersity index of Stokes radius <~30%). For calculation of r_H the dependence of solvent viscosity of aqueous solutions on GdnHCl concentration must be taken into account. This has been done on the basis of data provided by Kawahara and Tanford (*18*). The concentrations of the other solution components were sufficiently low so that their influence on viscosity could be neglected.

Analysis of GdnHCl and Urea Unfolding Equilibria. Denaturant unfolding curves were analyzed on the basis of two-state and three-state unfolding models. Two-state analysis (*5, 19–24*) was done according to well-known procedures and was found to be insufficient for a proper description of the unfolding reaction of His_6HodC69S. The sequential three-state model used in this study for the analysis of the transition curves is described in the following.

$$N \overset{K_{NI}}{\rightleftharpoons} I \overset{K_{ID}}{\rightleftharpoons} D \tag{5}$$

The equations relevant to thermal unfolding involving a three-state process have been given in the previous paper (*3*). Here we report the equations relevant to isothermal denaturant unfolding. We represent the observed signals of the various experimental techniques (CD, fluorescence, DLS) by x and assume that they are extensive (i.e., mass or concentration dependent). Each signal, x, observed as a function of denaturant concentration (GdnHCl or urea), c_{Denat}, is the weighted sum of the signals of the three pure states: the native state X_N, the intermediate state X_I, and the denatured state X_D shown in eq 6.

$$x = f_N X_N + f_I X_I + f_D X_D \tag{6}$$

Generally, it was found that the assumption of a linear dependence on denaturant concentration was sufficient for a proper analysis (*19, 21–24*). The linear relation is written for the native state X_N in eq 7, and analogous equations are valid for X_I and X_D.

$$X_N = X_N(H_2O) + c_{Denat}\left(\frac{dX_N}{dc_{Denat}}\right) \tag{7}$$

The fractions f_N, f_I, and f_D of native, intermediate, and denatured states of the protein in equilibrium were calculated using eqs 8−10.

$$f_N = \frac{1}{1 + K_{NI}(1 + K_{ID})} \tag{8}$$

$$f_I = \frac{K_{NI}}{1 + K_{NI}(1 + K_{ID})} \tag{9}$$

$$f_D = \frac{K_{NI}K_{ID}}{1 + K_{NI}(1 + K_{ID})} \tag{10}$$

The equilibrium constants are defined by the equations

$$K_{NI} = \exp\left(-\frac{\Delta G^o_{NI}}{RT}\right) \tag{11}$$

$$K_{ID} = \exp\left(-\frac{\Delta G^o_{ID}}{RT}\right) \tag{12}$$

where the standard Gibbs energy changes ΔG^o_{NI} and ΔG^o_{ID} are assumed to be linearly dependent on denaturant concentration.

$$\Delta G^o_{NI} = \Delta G^o_{NI}(H_2O) + \left(\frac{\partial \Delta G^o_{NI}}{\partial c_{Denat}}\right) c_{Denat} = \Delta G^o_{NI}(H_2O) + m_{NI} c_{Denat} \tag{13}$$

$$\Delta G^o_{ID} = \Delta G^o_{ID}(H_2O) + \left(\frac{\partial \Delta G^o_{ID}}{\partial c_{Denat}}\right) c_{Denat} = \Delta G^o_{ID}(H_2O) + m_{ID} c_{Denat} \tag{14}$$

$$\Delta G^o_{total} = \Delta G^o_{NI} + \Delta G^o_{ID} \tag{15}$$

m_{NI} and m_{ID} are the slopes of the corresponding standard Gibbs energy curves.

The overall stability is represented by the sum of the two standard Gibbs energy changes as shown in eq 15. The individual $c_{1/2}$ values of the N → I and I → D transitions can be obtained from the condition that at $c_{1/2}$ the standard Gibbs energy change is equal to zero, corresponding to an equilibrium constant $K = 1$. This leads to eqs 16 and 17.

$$\Delta G^{o}_{NI}(H_2O) = -m_{NI}c_{1/2,NI} \quad (16)$$

$$\Delta G^{o}_{ID}(H_2O) = -m_{ID}c_{1/2,ID} \quad (17)$$

RESULTS

Number of Disulfide Bridges in Native Protein. The amino acid sequence of Hod (accession no. CAL09864) indicates that the HodC69S protein contains two cysteine residues at positions 37 and 184. It is important to know whether under native conditions these thiol residues are reduced or whether they form a disulfide bridge. We probed this by applying Ellman's reagent and found that after unfolding by urea in the presence of $NaBH_4$ an OD change of 0.18 occurred indicative of DTNB reaction. According to eq 1 this is equivalent to two thiol groups becoming accessible to DTNB. This proves clearly the existence of a disulfide bond between Cys37 and Cys184 in the native protein.

Activity Studies. In the course of our studies various charges of freshly prepared protein were employed. However, each preparation of His_6HodC69S showed a specific activity of 70 units (mg of protein)$^{-1}$, indicating constant sample characteristics. Tests were made following the procedures given in ref *4* using phosphate buffer instead of the Tris buffer used in the original paper. We observed independent of the buffer system always a specific activity of 70 units mg^{-1} for the native protein.

A significant question concerns the correlation of catalytic activity with the degree of unfolding associated with the increase in denaturant concentration. Figure 1 shows the specific activity of His_6HodC69S as a function of denaturant concentration. Addition of GdnHCl results in an almost linear decrease of activity up to ~1 M where activity vanishes. Increasing concentrations of urea give rise to a nonlinear decrease of activity, and the activity is lost at approximately 5 M urea. It is worth noticing that the residual activity agrees well with the residual concentration of native protein at the respective denaturant concentrations.

CD-Monitored Unfolding Studies. (A) Unfolding by GdnHCl. Figure 2A shows the mean residue ellipticity at 222 nm of His_6HodC69S protein at 25 °C as a function of GdnHCl concentration. It is evident that unfolding of the protein does not proceed via a simple two-state transition but involves at least one intermediate state. This intuitive conclusion is fully corroborated by a three-state fit, which is shown graphically as the solid red curve. To keep the number of the fit parameters minimal, we assumed no higher than linear dependence of the MRE values on GdnHCl of both the native and the unfolded state.

There is no information on the variation of secondary structure of the intermediate state I with denaturant concentration. Therefore, we calculated with a constant MRE value of −5890 deg cm^2 dmol^{-1} as indicated by the dotted pink line. The lower part of Figure 2 shows the fractions of the three protein states as a function of denaturant concentration. The transition of the native to the intermediate state is highly cooperative ($c_{1/2} = 0.74$ M) and is characterized by a loss of about 80% of the ellipticity that is associated with complete unfolding. The transition from the intermediate state I to the unfolded state D exhibits lower cooperativity and has a $c_{1/2}$ value of 2.27 M. The mean residue ellipticity of −3200 deg cm^2 dmol^{-1} which is still present at 6 M GdnHCl suggests the existence of some residual secondary structure. This finding is in line with the occurrence of a disulfide bridge in native His_6HodC69S protein that is likely to retain some structure even at high denaturant concentrations (*25*). It is worth mentioning that, in comparison to thermal unfolding in buffer, denaturant action results in a significantly higher maximal percentage of the intermediate (60% for thermal unfolding compared to about 97% for denaturant unfolding). The maximal concentrations of the intermediate occur of course at different temperatures, a fact that relativizes the comparison of the percentages somewhat. The corresponding GdnHCl concentration, at which the intermediate concentration is maximal, is ~1.4 M. At this concentration both native structure and activity have vanished. Those findings lead to the conclusion that the intermediate state of the protein has no enzyme activity under these conditions.

(B) Unfolding by Urea. In view of the frequently observed differences between thermodynamic parameters derived from GdnHCl and urea unfolding for the same protein (*5–7*) we performed also urea unfolding studies with His_6HodC69S. Conformational changes were observed by CD at 222 and 295 nm to follow changes in secondary and tertiary structure. Inspection of the curves shown in Figure 2B would not immediately imply three-state unfolding, and indeed, the experimental MRE data can be fitted reasonably well assuming two-state behavior. The extrapolated standard Gibbs energy change, $\Delta G°$, at zero urea concentration is 40 ± 2 kJ mol^{-1} for the two-state transition. However, in view of the results obtained with GdnHCl and the strong evidence of three-state unfolding provided by our previous studies (*3*) as well as by the present fluorescence and DLS measurements discussed below, we inferred also three-state unfolding for denaturation by urea. We used the $c_{1/2}$ values obtained from the three-state fits of the fluorescence studies as starting parameters for the fits of the CD-monitored urea transition curves. The good representation of the CD data at 222 nm by the fitted curve is obvious in the graph. However, it is also evident on inspection of the thermodynamic parameters presented in Table 1 that the partition of the overall standard Gibbs energy change between the N−I and I−D transitions differs from that of all the others. This results from the pronounced two-state character of the transition curve which favors the first transition over the second.

When applying the same fit strategy to the transition curve observed at 295 nm, a three-state transition model does not improve the quality of the fit compared to a two-state model. Both model calculations yield a $c_{1/2}$ value of about 3 M urea, which is practically identical to the $c_{1/2}$ value of 2.9 M obtained for the N → I transition observed at 222 nm.

Fluorescence Measurements. Changes in fluorescence emission intensity and λ_{max} shifts are sensitive measures of changes in exposure to solvent of tryptophans and tyrosines resulting from alterations of tertiary structure. We performed

Table 1: Comparison of Thermodynamic Parameters for GdnHCl- and Urea-Induced Unfolding of His_6HodC69S in 10 mM Sodium Phosphate and 10 mM Sodium Borate, pH 7.5, at 25 °C[a]

observed property	$\Delta G^{\circ}_{NI}(H_2O)$ (kJ mol^{-1})	m_{NI} (kJ mol^{-1} M^{-1})	$c_{1/2,NI}$ (M)	$\Delta G^{\circ}_{ID}(H_2O)$ (kJ mol^{-1})	m_{ID} (kJ mol^{-1} M^{-1})	$c_{1/2,ID}$ (M)
			GdnHCl Denaturation			
CD (222 nm)	12.3 ± 1.5	−16.6 ± 2.0	0.74 ± 0.02	25.8 ± 12	−11.4 ± 5.4	2.27 ± 0.1
fluorescence intensity[c]	13.2 ± 3.9	−19.5 ± 5.1	0.68 ± 0.04	25.1 ± 3.9	−11.1 ± 1.8	2.27 ± 0.04
λ_{max} shift	13.0 ± 1.1	−17.2 ± 1.4	0.76 ± 0.01	26.1 ± 3.8	−12.9 ± 1.8	2.02 ± 0.03
DLS (r_H)	14.8 ± 1.3	−14.3 ± 1.2	1.03 ± 0.02	27.0 ± 8.3	−11.1 ± 3.6	2.43 ± 0.08
			Urea Denaturation			
CD (222 nm)	20.5 ± 2.5	−7.1 ± 0.9	2.9 ± 0.2	22.0 ± 12	−4.0 ± 2.3	5.5 ± 0.9
CD (295 nm)[b]	39.7 ± 4.7	−13.1 ± 1.5	3.0 ± 0.02			
fluorescence intensity[c]	13.3 ± 1.2	−4.6 ± 0.4	2.92 ± 0.04	27.9 ± 8.7	−5.0 ± 1.5	5.6 ± 0.2
λ_{max} shift	15.0 ± 1.5	−5.03 ± 0.04	2.98 ± 0.04	27.2 ± 16.6	−4.5 ± 2.5	6.1 ± 0.33
			Heat Denaturation			
	$T_{m,NI}$ (K)	$\Delta H(T_{m,NI})$ (kJ mol^{-1})	$\Delta C_p(T_{m,NI})$ (kJ mol^{-1} K^{-1})	$T_{m,ID}$ (K)	$\Delta H(T_{m,ID})$ (kJ mol^{-1})	$\Delta C_p(T_{m,ID})$ (kJ mol^{-1} K^{-1})
CD (222 nm) ox. Hod	325.6	257	11.3	330.7	475	6.7
CD (222 nm) red. Hod	314.1	261	10.3	320.4	458	6.7

[a] Evaluation was based on the three-state model described by eqs 5−17. [b] Parameters refer to two-state analysis. [c] Excitation wavelength 295 nm and emission wavelength 350 nm.

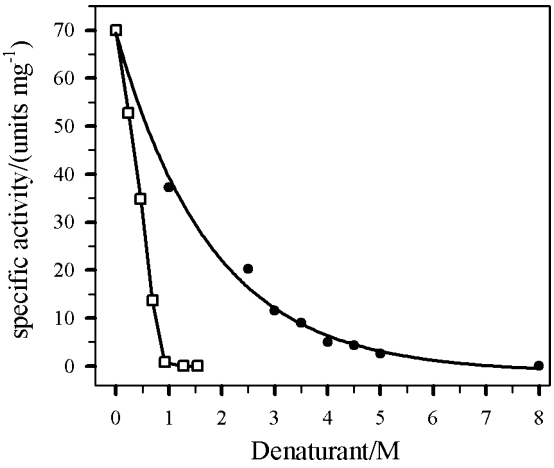

FIGURE 1: Specific activity of His_6HodC69S as a function of denaturant concentration: (□) specific activity as a function of [GdnHCl]; (●) specific activity as a function of [urea]. The solid lines are only guidelines for the eye.

such measurements on His_6HodC69S as a function of both GdnHCl and urea concentration. The results are shown in Figure 3. It is obvious that all transition curves show non-two-state behavior, independent of the method of detection (intensity or λ_{max}) and independent of the denaturant used for unfolding. Furthermore, the Gibbs energies resulting from the three-state fits are within rather narrow error limits identical, as the summary in Table 1 demonstrates.

Fluorescence intensity is closely linked to changes in exposure of the fluorescent residues to solvent. Therefore, it mirrors sensitively local changes of tertiary structure. The graphs shown in Figure 3A,C reflect the differences in unfolding power of GdnHCl and urea but also the similarities of the unfolding sequence. The standard Gibbs energy changes observed for the N → I and I → D transitions agree well, independent of whether the transition was caused by GdnHCl or urea. The corresponding ΔG° values for the N → I transition are $\Delta G^{\circ}_{NI}(H_2O) = 13.2$ kJ mol^{-1} (for GdnHCl unfolding) and $\Delta G^{\circ}_{NI}(H_2O) = 13.3$ kJ mol^{-1} (from urea unfolding); those for the I → D transition are $\Delta G^{\circ}_{ID}(H_2O) = 25.1$ kJ mol^{-1} and $\Delta G^{\circ}_{ID}(H_2O) = 27.9$ kJ mol^{-1}.

In contrast to the changes in emission intensity the shifts in λ_{max} with increasing denaturant concentration cannot be directly or unequivocally related to molecular details as discussed by Eftink (*26*), Monsellier and Bedouelle (*27*), Ewert et al. (*28*), and Duy and Fitter (*29*). Particularly, it cannot generally be expected that λ_{max} shifts reflect linearly the mole fraction of states. However, it can be shown that, under special spectral conditions, these data can be used to evaluate the true thermodynamic parameters (*26*). The constraints are (1) the half-width of the emission peaks of all three states should remain nearly constant, (2) the maximal intensity should not change drastically, and (3) the λ_{max} shift should not exceed the half-width of the spectrum. These conditions are met by our emission spectra. A pronounced advantage of the λ_{max} shift data in relation to the intensity is the much smaller scattering of the values due to deviations in the protein concentration. Therefore, we can expect to obtain similar thermodynamic parameters from fitting λ_{max} as a function of denaturant concentration as from fitting intensity. Table 1 shows that, within error limits, similar standard Gibbs energy values are indeed obtained from both transition curves.

A closer look at the variations with GdnHCl concentration of fluorescence intensity reveals some interesting aspects. Increasing GdnHCl concentration in the native state region of the enzyme induces a decrease in fluorescence intensity. Above about 0.6 M GdnHCl, intensity begins to rise, and it reaches a maximum at approximately 1.3 M. At this denaturant concentration the maximal degree of intermediate is present. Further increase of GdnHCl concentration results in progressive unfolding and concomitant decrease of emission intensity. When the protein is fully unfolded, further increase of GdnHCl concentration is associated with moderate linear increase in fluorescence intensity. Obviously this complex pattern of fluorescence changes needs further explanation.

The first linear decrease in intensity up to ~0.4 M GdnHCl is not associated with a λ_{max} shift, as Figure 3B shows. Therefore, it is probably not caused by changes in the hydration of the tryptophans but rather indicates an increase

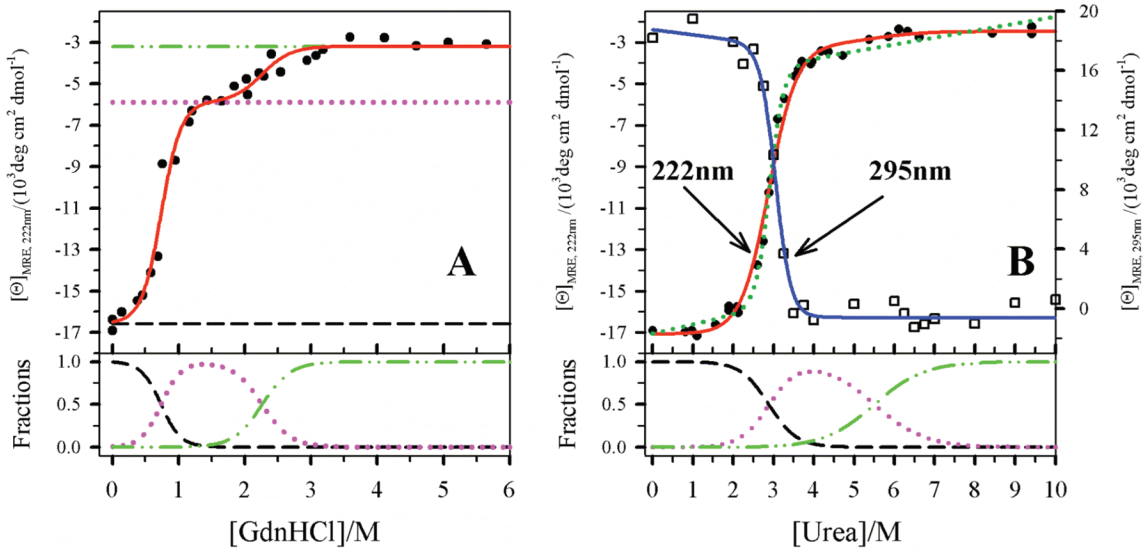

FIGURE 2: CD-monitored chemical denaturation of His_6HodC69S protein at 25 °C. The protein concentration was 1 mg mL^{-1}, and the buffer was 10 mM sodium phosphate and 10 mM sodium borate, pH 7.5. Key: (●) experimental data; (red solid curves) three-state fit; (black dashed curves) native state; (pink dotted curves) intermediate state; (green dashed-dotted curves) denatured state. Data analysis was based on the sequential three-state model (eqs 6−17). The relevant thermodynamic parameters are summarized in Table 1, and detailed information is given in the Supporting Information. The lower panels of the graphs display the fractions of native, intermediate, and denatured states as a function of GdnHCl concentration. (A) GdnHCl-induced unfolding observed at 222 nm. (B) Urea-induced unfolding observed at 222 nm (●) or 295 nm (□). The protein concentration was 0.5 mg mL^{-1}. Unfolding at 222 nm: (●) experimental data; (red solid curve) fit curve, three-state model fit; (dotted dark green curve) two-state fit. Unfolding at 295 nm: (□) experimental data; (blue solid curve) two-state fit. The baselines were left out in panel B to avoid crowding of the graph. The fraction curves of the two-state analysis are not shown. They have nearly the same value of $c_{1/2}$ as the N−I transition.

in quenching of neighboring tryptophans, tyrosines, histidines, or disulfide residues, as suggested previously (*30–35*).

At GdnHCl concentrations higher than ~0.4 M the degree of exposure of tryptophans increases cooperatively, as the shift of λ_{max} suggests. This process is accompanied by an increase in fluorescence intensity, which can be rationalized by a reduction of quenching resulting from the perturbation of the native structure. The pattern of fluorescence changes seen with urea as denaturant is analogous to that observed with GdnHCl. This is shown in Figure 3C,D. Between 0 and 1.5 M urea, fluorescence intensity of the native protein decreases also linearly but less strongly. With the appearance of the intermediate state I fluorescence increases, remains at similar level between 4 and 6 M urea, and shows a linear increase with increasing urea concentration above 7 M, where about 90% of the protein is denatured. Thus the general pattern of the λ_{max} shift as a function of the urea concentration also resembles that obtained with GdnHCl as denaturant. Quantitative differences show up in the $c_{1/2}$ values which occur in the presence of urea of course at higher denaturant concentration.

In view of the similarities of the GdnHCl and urea transition curves we infer that the same mechanism of fluorescence changes is operative in both denaturant systems. This interpretation gains support from DLS determinations of Stokes radii as a function of GdnHCl concentration. DLS permits to measure sensitively changes in the diffusion coefficient of the protein resulting from conformational changes concomitant with denaturant unfolding and/or binding. The changes in Stokes radius of His_6HodC69S protein observed with increasing GdnHCl concentration are summarized in Figure 4.

The experimentally observed Stokes radii can be represented well by a fitting curve based on the three-state model and the same energy parameters of unfolding as used before in the fits of the fluorescence data (Table 1).

Inspection of Figure 4 shows that the dimensions of the native protein do not appear to change between 0 and 0.4 M GdnHCl in accordance with the constancy of λ_{max}. They are, however, cooperatively increased when the intermediate is formed and remain approximately constant between 1.5 and 2.5 M GdnHCl. Further increase in GdnHCl concentration unfolding is reflected in an apparently linear increase of the Stokes radius of the protein. A similar expansion has been observed by Baskakov and Bolen when studying urea unfolding of *Staphylococcus* nuclease protein (*36*).

Summarizing all results, one can draw the important conclusion that different physical parameters such as heat capacity, fluorescence intensity, λ_{max} shifts, and Stokes radii provide a consistent picture of the mechanism of equilibrium unfolding of His_6HodC69S. The native state passes through an intermediate before it fully unfolds, and a unique set of thermodynamic parameters describes the various transition curves monitored by different techniques.

Thermal Unfolding of Oxidized and Reduced Protein (CD Studies). To quantify the stabilizing effect of the C37−C184 disulfide bond on the native structure, we performed CD-monitored heating scans of both the oxidized and reduced protein. The results are shown in Figure 5. Two characteristic differences are evident on inspection. The total change in ellipticity of the reduced protein is smaller than that of the native oxidized protein, and the midpoint of the transition is shifted to lower temperatures by approximately 11 degrees. Because the transition curves are practically parallel, the transition enthalpies are also similar, as the quantitative three-state analysis shows. The overall Gibbs energy difference between the oxidized and reduced protein at 25 °C, that could

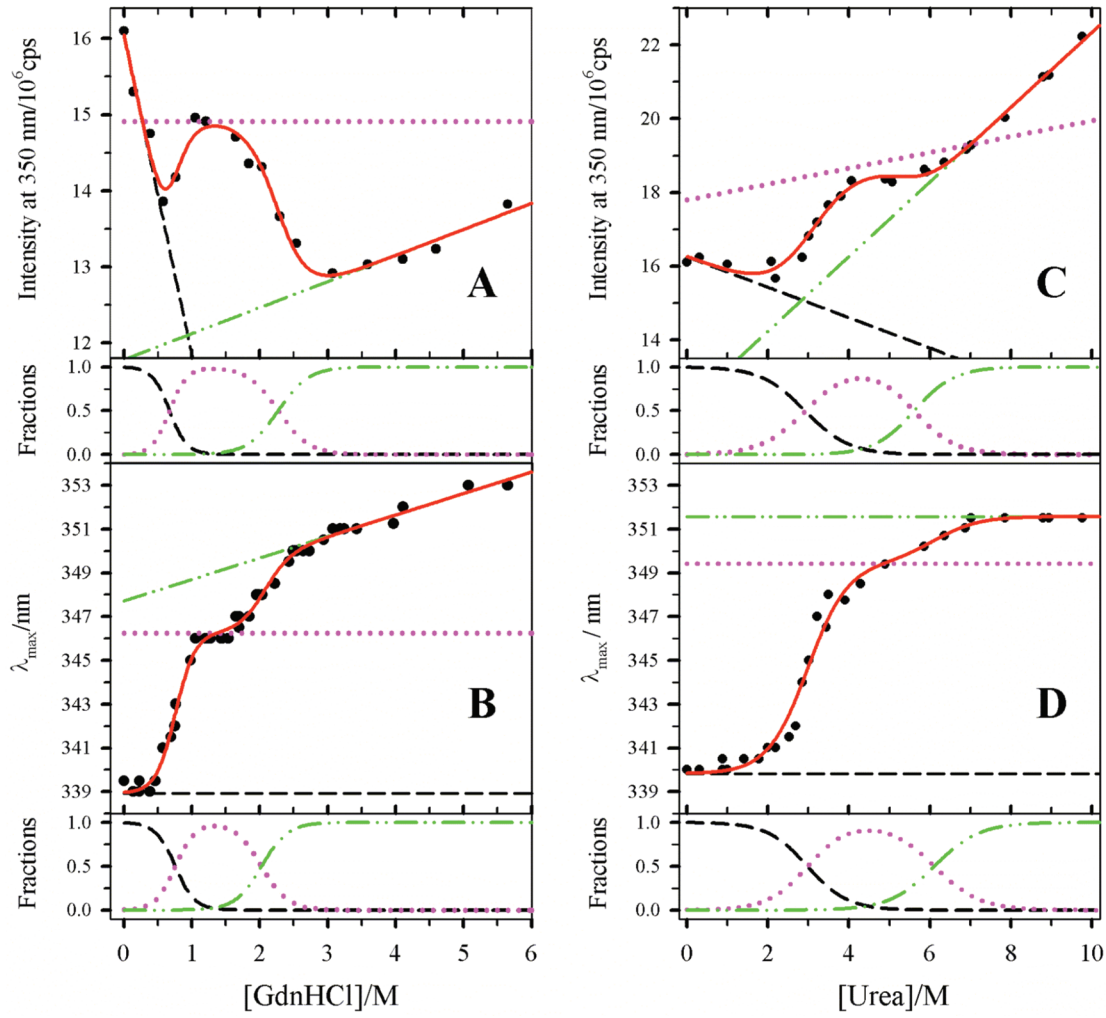

FIGURE 3: Fluorescence emission intensity at 350 nm (A, C) and λ_{max} shifts (B, D) of His_6HodC69S as a function of GdnHCl (A, B) or urea (C, D) concentration at 25 °C. Protein concentration was 0.05 mg mL^{-1} in all measurements. Buffer: 10 mM sodium phosphate and 10 mM sodium borate, pH 7.5. Key: (●) experimental data; (red solid curves) fit curve; (black dashed curves) native state; (pink dotted curves) intermediate state; (green dashed-dotted curves) denatured state. All data were analyzed using the sequential three-state model (eqs 6−17). The relevant thermodynamic parameters are summarized in Table 1, and detailed information is given in the Supporting Information. The lower panels of the graphs display the fractions of native, intermediate, and denatured states as a function of denaturant concentration.

be assigned to the contribution of the disulfide bond, is about $\Delta\Delta G° = 10 \pm 2$ kJ mol^{-1}.

A detailed thermodynamic analysis using the equations given in our previous publication (*3*) provides also the standard Gibbs energy changes at the corresponding transition temperatures of the N−I and I−D transitions of the native and reduced protein. Relative to the transition temperatures of the native protein containing the disulfide bond one obtains the following stability differences: $\Delta\Delta G°(52.4\ °C)_{Ox,NI} = 11.7$ kJ mol^{-1}; $\Delta\Delta G°(57.5\ °C)_{Ox,ID} = 14.1$ kJ mol^{-1}. These $\Delta\Delta G°$ values can be compared to estimates of stability changes based on changes of transition temperature first suggested by Becktel and Schellman (37).

Their method implies that (a) the stability curves of the native and modified protein are parallel in the relevant temperature range of the shift (approximation of ΔS(perturbed) by ΔS(native)) and (b) the curvature of the stability curve is negligible around this temperature. Under these assumptions the following equation provides the stability difference.

$$\Delta\Delta G° = \frac{\Delta T_m \Delta H(T_m)}{T_m} \qquad (18)$$

$\Delta T_m = T_{m,NI,Ox} - T_{m,NI,Red}$ or $\Delta T_m = T_{m,ID,Ox} - T_{m,ID,Red}$ are the differences in transition temperatures for the N−I and I−D transitions of the oxidized and reduced proteins. $\Delta H(T_m)$ refers to the enthalpies of the two subtransitions N−I and I−D of the native oxidized His_6HodC69S protein. The stability differences at the transition temperatures of the native protein resulting from application of eq 18 are $\Delta\Delta G°(52.4\ °C)_{Ox,NI} = 9.1$ kJ mol^{-1} and $\Delta\Delta G°(57.5\ °C)_{Ox,ID} = 14.8$ kJ mol^{-1}. In view of the assumptions that enter the estimates the agreement is good.

DISCUSSION

The present isothermal urea and GdnHCl unfolding studies provide conclusive evidence that the fairly large monomeric His_6HodC69S protein (M = 33240.4 g mol^{-1}) is characterized by reversible cooperative three-state unfolding and that the thermodynamic parameters governing the transitions are within experimental error the same as those determined in a previous investigation from DSC measurements and various spectroscopic transition curves in the absence of denaturants. Such universality of thermodynamic transition properties can be expected in principle but has seldom been demonstrated

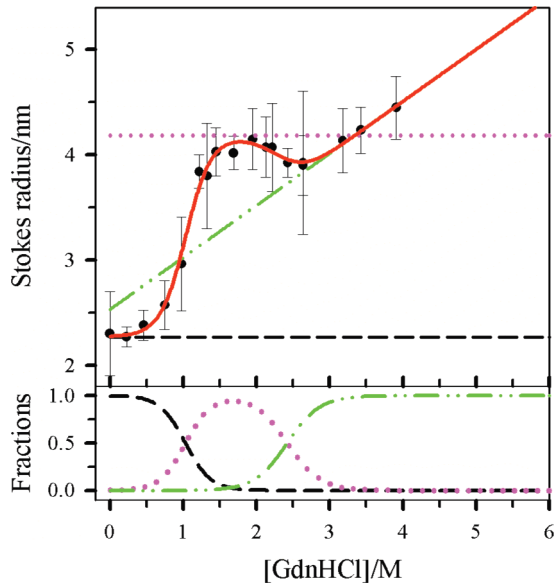

FIGURE 4: Dynamic light scattering measurements of denaturation of the His_6HodC69S protein with GdnHCl at 25 °C. The buffer was 10 mM sodium phosphate and 10 mM sodium borate, pH 7.5. Two protein concentrations were measured, 0.05 and 1 mg mL^{-1}, with identical results. The data points represent values averaged over 10−30 acquisitions, depending on the quality of the data; bars indicate standard deviations. Key: (●) experimental data; (red solid line) fit curve; (black dashed curves) native state; (pink dotted curves) intermediate state; (green dashed-dotted curves) denatured state. Data analysis was made on the basis of the sequential three-state model. The derived thermodynamic parameters are summarized in Table 1, and signal parameters are shown in the Supporting Information.

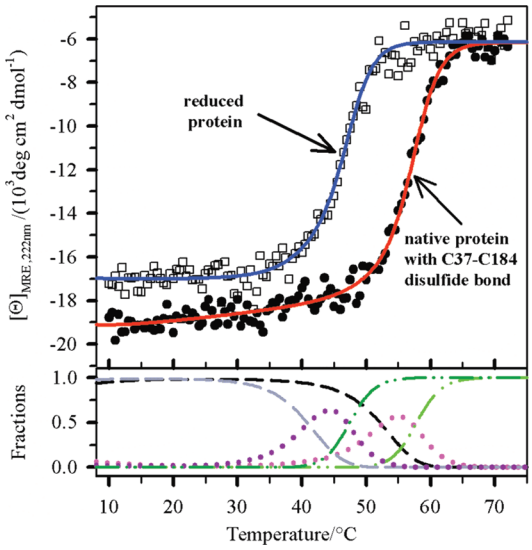

FIGURE 5: CD transition curves of His_6HodC69S as isolated (filled symbols) and after reduction with 40 mM dithiothreitol (open squares). The protein concentration was 1 mg mL^{-1} in 10 mM sodium phosphate and 10 mM sodium borate buffer, pH 7.5; the heating rate was $r = 1.0$ K min^{-1}. Solid curves represent fits to the sequential three-state model. The thermodynamic parameters are given in Table 1, and detailed information is presented in the Supporting Information. The average shift in T_m is ∼11 °C. The overall stability at 25 °C of the reduced protein is $\Delta G° = 31.8$ kJ mol^{-1}.

by such a plethora of denaturation and observation techniques on the same system as in the present study.

The native state of the protein has a Stokes radius of 2.3 ± 0.4 nm at 25 °C which has been shown to remain constant in aqueous buffer solution, pH 7.5, until a temperature of approximately 40 °C is reached (*3*). Above that temperature thermal unfolding is initiated and heterogeneity of the protein appears. Therefore, it was not possible to determine the Stokes radius of the thermally unfolded protein. This prompted us to endeavor DLS studies as a function of GdnHCl concentration in order to see whether the three conformational states observed in thermal unfolding studies could be identified also in denaturant unfolding studies by their degree of expansion. Such an analysis is complementary to information gleaned from CD and fluorescence studies, as the interactions responsible for maintenance of the native state and phenomena such as fluorescence quenching or activity are of short-range character and therefore highly distance-dependent.

Activity and Structure. When comparing the loss of catalytic activity as a function of GdnHCl or urea concentration given in Figure 1 with the disappearance of secondary and tertiary structure shown in Figures 2 and 3, it is evident that neither the intermediate nor the unfolded states show any enzymatic activity. In GdnHCl solution this is very obvious. At 1.3 M denaturant, in the presence of the maximal percentage of the intermediate and practically zero percentage of the unfolded state, activity is abolished. The situation with urea is somewhat more complex. Activity is lost at about 4.5−5 M urea. Tertiary structure, as evidenced by the transition curve monitored at 295 nm, is disrupted at approximately 4 M urea. Secondary structure is apparently present with significant fractions of the intermediate at 4.5 to 5 M as shown by the 222 nm CD absorption. This could suggest that the intermediate state would exhibit some residual activity. However, we do not consider this inference very likely. Fluorescence intensity as well as λ_{max} shift indicate that the native state structure is lost at about 4 M urea.

Activity and Stokes Radius. An interesting aspect is revealed when the disappearance of enzymatic activity in GdnHCl solution is related to the expansion of the protein. At 1 M GdnHCl, where activity has vanished, the Stokes radius has increased from 2.3 to about 3 nm. Inspection of the changes with GdnHCl concentration of Stokes radius of His_6HodC69S protein shown in Figure 4 provides suggestive evidence that this transition curve cannot be fitted to a two-state model. It can, however, be represented excellently by a three-state fit, as demonstrated by the solid red line. The $c_{1/2}$ value obtained for the N → I transition is larger than that derived from the spectroscopic techniques (by about 40%). This is in principle not surprising, as it cannot be expected that those properties of the intermediate state of the protein which are reflected in changes of the diffusion coefficient (and therefore in the Stokes radius) are to the same degree visible in changes of fluorescence or CD. The most important result is thus not the coincidence of $c_{1/2}$ values but the very appearance of more than two states in the course of unfolding.

It is another noteworthy result of the DLS study that the Stokes radius of unfolded His_6HodC69S protein increases linearly with GdnHCl concentration. The linear extrapolation to zero molar denaturant provides a Stokes radius for the unfolded protein of approximately 2.6 nm. This estimate is in good agreement with the values of about 3 nm at 57 °C

reported in our previous thermal unfolding measurements in buffer (*3*).

Comparison of Experimental and Theoretical Stokes Radii. Uversky (*38*) has reported a summary of Stokes radii of native and of completely unfolded proteins having molar monomer masses between 3000 and 165000 g mol^{-1}. Using his relation between Stokes radius and molar mass, one obtains for His_6HodC69S (M = 33240.4 g mol^{-1}) a native state radius of 2.5 nm and an unfolded state radius of 5.3 nm which agrees well with our findings for 6 M GdnHCl. Another estimate can be obtained using equations reported by Wilkins et al. (*39*) and Damaschun et al. (*40*). The Stokes radii calculated according to ref *39* are 2.45 ± 0.8 nm for the native protein and 5.57 ± 2.6 nm for the unfolded protein. When using the equations suggested by Damaschun (*40*), one obtains 4.75 ± 1 nm for the unfolded state. Geierhaas et al. (*41*) provide a method for the calculation of the change in the radius of gyration (*42*), R_G, as a function of the number of the amino acid residues. It is based on a relationship, eq 19, introduced originally by Flory (*43*)

$$R_G = R_0 N^{\upsilon} \tag{19}$$

in which R_0 is a constant related to the persistence length of the protein and υ is an exponent that describes how R_G scales with the length N of the protein. Kohn et al. (*44*) report the following values: R_0 = 2.08 ± 0.19 Å and υ = 0.598 ± 0.029. The value for υ agrees fairly well with the theoretical value of υ = 0.6 reported by Flory (*43*), the value υ = 0.588 applied by LeGuillou and Zinn-Justin (*45*) as well as that used by Geierhaas et al. (*41*), υ = 0.61.

Application of eq 19 to His_6HodC69S protein with N = 288, R_0 = 2.07 Å, and υ = 0.61 results in a radius of gyration for the unfolded protein of 6.6 nm. The change in R_G on unfolding was calculated using eq 13 of Geierhaas et al. (*41*). We obtained ΔR_G = 5.1 ± 0.3 nm. Subtraction of this number from R_G = 6.6 nm yields the radius of gyration of the native protein. The Stokes radius of the native protein was obtained from the equation $r_H = R_G/\rho$, where $\rho = 8/(3(\pi)^{1/2})$ is the value for monodisperse linear chains and $\rho = (3/5)^{1/2}$ is the parameter for spheres. We considered this latter value of ρ appropriate for the calculation of the radius of native proteins. For native His_6HodC69S one obtains approximately $r_{H,native} \simeq 2$ nm and for the unfolded species $r_{H,unfolded} \simeq 4.37$ nm.

In summary, we can state that the Stokes radii obtained from DLS measurements agree well with those predicted on the basis of polymer science.

Fluorescence Changes and Structure. The fluorescence intensity and λ_{max} shift data reflect local structural changes of the protein resulting from changes in denaturant concentration. It is evident that we cannot assume a priori that the various techniques, such as fluorescence, CD (222 nm), CD (295 nm), and DLS, provide the same information. This is partly due to the fact that local changes associated with the N → I or I → D transitions are likely to be monitored differently by the various observation techniques. For example, one can assume that, due to the excitation at 295 nm, fluorescence intensity probes preferentially local arrangements of the nine tryptophans as a function of denaturant concentration. In contrast, CD at 295 nm and DLS reflect predominantly alterations in the overall tertiary structure. This difference in informational content is particularly obvious in the CD (295 nm) transition curve, which can be fitted as well to a two-state as to a three-state model. In all other cases the observed data permit no convincing alternative to three-state fitting.

Inspection of the changes in fluorescence emission as a function of GdnHCl or urea concentration shown in Figure 3A,C reveals a decrease with increasing denaturant concentration. This decrease is larger than that observed with pure tryptophan solutions (*46*). Therefore, it could be assumed that from 0 to 0.4 M GdnHCl or 0 to 1.5 M urea the denaturants cause conformational changes which result in increased quenching of tryptophan fluorescence. The constancy of λ_{max}, CD signals, and Stokes radius in the presence of these low GdnHCl or urea concentrations is evident in Figures 2, 3B,D, and 4. These results support the view that the structural changes reflected in the changes of tryptophan fluorescence intensity at low denaturant concentrations involve not more than 10% of the N → I transition. Among the various mechanisms that can be invoked for fluorescence quenching (*30–35, 47–50*) we favor quenching by the disulfide bridge formed between cysteine residues C37 and C184. This requires of course the occurrence of some of the tryptophans within a distance of approximately 10−15 Å to the disulfide bridge for the quenching mechanisms to become operative. In contrast to proton transfer it has less stringent geometric constraints and can be effective over a distance of more than 10 Å. It is therefore likely to be a major quenching mechanism in peptides and proteins (*30*). The observed decrease in fluorescence (Figure 3A) associated with the increase in GdnHCl concentration from 0 to 0.4 M could therefore be assigned to excited electron transfer facilitated by proximity, specific geometry, and local polarity of the disulfide group and various tryptophans.

When such structural arrangements characteristic of the native state ensemble are perturbed in the course of the N → I transition, relative distances and orientations are changed significantly, as seen by the DLS transition curve. As a result quenching becomes less efficient and fluorescence emission intensity increases to a maximum at about 1.4 M GdnHCl. The further decrease of fluorescence associated with the increase in GdnHCl concentration to 3 M is predominantly a consequence of the red shift of λ_{max}, as the maximum of the emission spectrum remains constant. If the λ_{max} shift is reflecting an increase in the degree of exposure to solvent of hydrophobic residues, both the CD (222 nm) evidence (Figure 2) and the Stokes radii (Figure 4) indicate only minor changes between 1.4 and 3 M. Thus the increased accessibility to solvent of the structure of the intermediate is not associated with a further expansion of the protein.

Above 3 M GdnHCl one observes a linear increase in both Stokes radius and fluorescence intensity. The changes seen in Stokes radius could be interpreted as additional swelling of the protein molecule (*36*). However, they might also be due to additional binding of GdnHCl molecules with concomitant changes in the diffusion coefficient (*51*). In this case the changes of Stokes radius should be termed "apparent" as they result from increases in molar mass rather than expansion. The linear increase in fluorescence intensity of His_6HodC69S protein observed above 3 M GdnHCl is rather similar to that reported for aqueous tryptophan solutions (*46*).

It is therefore not indicative of additional structural changes resulting from the increase in denaturant concentration.

CONCLUSIONS

The present isothermal denaturant unfolding studies of His_6HodC69S provide a convincing argument in favor of the universality of the thermodynamic characterization of protein unfolding. Despite significant differences in the shapes of the unfolding curves monitored by different probes such as CD, fluorescence, dynamic light scattering, or heat capacity, all transition curves could be analyzed consistently on the basis of a three-state mechanism N = I = D. Very similar sets of thermodynamic parameters could be used for the description of both temperature and denaturant-induced unfolding. The universality of the thermodynamic approach is based on the reversibility of both thermal and chemical unfolding processes of this protein.

ACKNOWLEDGMENT

We are grateful to Dr. R. Steiner (London) for access to structural information on the protein prior to publication. It was reassuring that our interpretation of the spectroscopic data was fully consistent with structural evidence.

SUPPORTING INFORMATION AVAILABLE

Equations as well as spectroscopic and thermodynamic parameters employed in the fitting routines. This material is available free of charge via the Internet at http://pubs.acs.org.

REFERENCES

1. Fischer, F., Künne, S., and Fetzner, S. (1999) Bacterial 2,4-dioxygenases: New members of the α/β hydrolase-fold superfamily of enzymes functionally related to serine hydrolases. *J. Bacteriol. 181*, 5725–5733.
2. Fetzner, S. (2002) Oxygenases without requirement for cofactors or metal ions. *Appl. Microbiol. Biotechnol. 60*, 243–257.
3. Beermann, B., Guddorf, J., Boehm, K., Albers, A., Kolkenbrock, S., Fetzner, S., and Hinz, H.-J. (2007) Stability, unfolding, and structural changes of cofactor-free 1H-3-hydroxy-4-oxoquinaldine 2,4-dioxygenase. *Biochemistry 46*, 4241–4249.
4. Frerichs-Deeken, U., Ranguelova, K., Kappl, R., Hüttermann, J., and Fetzner, S. (2004) Dioxygenases without requirement for cofactors and their chemical model reaction: Compulsory order ternary complex mechanism of 1-*H*-3-hydroxy-4-oxoquinaldine 2,4-dioxygenase involving general base catalysis by histidine 251 and single-electron oxidation of the substrate dianion. *Biochemistry 43*, 14485–14499.
5. Ferreon, A. C. M., and Bolen, D. W. (2004) Thermodynamics of denaturant-induced unfolding of a protein that exhibits variable two-state denaturation. *Biochemistry 43*, 13357–13369.
6. Bolen, D. W., and Yang, M. (2000) Effects of guanidine hydrochloride on the proton inventory of proteins: implications on interpretations of protein stability. *Biochemistry 39*, 15208–15216.
7. Makhatadze, G. I. (1999) Thermodynamics of protein interactions with urea and guanidinium hydrochloride. *J. Phys. Chem. B 103*, 4781–4785.
8. Ramprakash, J., Doseeva, V., Galkin, A., Krajewski, W., Muthukumar, L., Pullalarevu, S., Demirkan, E., Herzberg, O., Moult, J., and Schwarz, F. P. (2008) Comparison of the chemical and thermal denaturation of proteins by a two-state transition model. *Anal. Biochem. 374*, 221–230.
9. Swint, L., and Robertson, A. D. (1993) Thermodynamics of unfolding for turkey ovomucoid third domain: Thermal and chemical denaturation. *Protein Sci. 2*, 2037–2049.
10. Carra, J. H., and Privalov, P. L. (1995) Energetics of denaturation and m values of staphylococcal nuclease mutants. *Biochemistry 34*, 2034–2041.
11. Eiden, F., Wendt, R., and Fenner, H. (1978) Chinolyliden-Derivate. *Arch. Pharm. (Weinheim, Ger.) 311*, 561–568.
12. Cornforth, J. W., and James, A. T. (1956) Structure of a naturally occurring antagonist of dihydrostreptomycin. *Biochem. J. 63*, 124–130.
13. Pace, C. N., Vajdos, F., Fee, L., Grimsley, G., and Gray, T. (1995) How to measure and predict the molar absorption coefficient of a protein. *Protein Sci. 4*, 2411–2423.
14. Ellman, G. L. (1959) Tissue sulfhydryl groups. *Arch. Biochem. Biophys. 82*, 70–77.
15. Baker, W. L., and Panow, A. (1991) Disulfide groups in proteins. *Biochem. Educ. 19*, 152–154.
16. Nozaki, Y. (1972) The preparation of guanidine hydrochloride. *Methods Enzymol. 26*, 43–50.
17. Warren, J. R., and Gordon, A. (1966) On the refractive indices of aqueous solutions of urea. *J. Phys. Chem. 70*, 297–300.
18. Kawahara, K., and Tanford, C. (1966) Viscosity and density of aqueous solutions of urea and guanidine hydrochloride. *J. Biol. Chem. 241*, 3228–3232.
19. Greene, R. F., and Pace, C. N. (1974) Urea and guanidine hydrochloride denaturation of ribonuclease, lysozyme, α-chymotrypsin and β-lactoglobulin. *J. Biol. Chem. 249*, 5388–5393.
20. Pace, C. N., and Vanderburg, K. E. (1979) Determining globular protein stability: guanidine hydrochloride denaturation of myoglobin. *Biochemistry 18*, 288–292.
21. Pace, C. N. (1986) Determination and analysis of urea and guanidinium hydrochloride denaturation curves. *Methods Enzymol. 131*, 266–280.
22. Pace, C. N., Shirley, B. A., and Thomson, J. A. (1989) Measuring the conformational stability of a protein, in *Protein Structure: A Practical Approach* (Creighton, T. E., Ed.) pp 311−330, IRL Press, Oxford.
23. Eftink, M. R., Ghiron, C. A., Kautz, R. A., and Fox, R. O. (1991) Fluorescence and conformational stability studies of *Staphylococcus* nuclease and its mutants, including the less stable nuclease-concanavalin A hybrids. *Biochemistry 30*, 1193–1199.
24. Aune, K. C., and Tanford, C. (1969) Thermodynamics of the denaturation of lysozyme by guanidine hydrochloride. II. Dependence on denaturant concentration at 25°C. *Biochemistry 8*, 4586–4590.
25. Hu, C. H., Zou, C., and Tsou, C. (1992) Disulfide-containing proteins denatured in 6 mol/L guanidinium chloride are not completely unfolded. *Sci. China, Ser. B 35*, 1214–1221.
26. Eftink, M. R. (1994) The use of fluorescence methods to monitor unfolding transitions in proteins. *Biophys. J. 66*, 482–501.
27. Monsellier, E., and Bedouelle, H. (2005) Quantitative measurement of protein stability from unfolding equilibria monitored with the fluorescence maximum wavelength. *Protein Eng. Des. Sel. 18*, 445–456.
28. Ewert, S., Honegger, A., and Plückthun, A. (2003) Structure-based improvement of the biophysical properties of immunoglobulin V_H domains with a generalizable approach. *Biochemistry 42*, 1517–1528.
29. Duy, C., and Fitter, J. (2006) How aggregation and conformational scrambling on unfolded states govern fluorescence emission spectra. *Biophys. J. 90*, 3704–3711.
30. Chen, Y., and Barkley, M. D. (1998) Toward understanding tryptophan fluorescence in proteins. *Biochemistry 37*, 9976–9982.
31. Cowgill, R. W. (1967) Fluorescence and protein structure, XI. Fluorescence quenching by disulfide and sulfhydryl groups. *Biochim. Biophys. Acta 140*, 37–44.
32. Azuaga, A. I., Canet, D., Smeenk, G., Berends, R., Titgemeijer, F., Duurkens, R., Mateo, P. L., Scheek, R. M., Robillard, G. T., Dobson, C. M., and van Nuland, N. A. J. (2003) Characterization of single-tryptophan mutants of histidine-containing phosphocarrier protein: Evidence for local rearrangements during folding from high concentrations of denaturant. *Biochemistry 42*, 4883–4895.
33. Hennecke, J., Sillen, A., Huber-Wunderlich, M., Engelborghs, Y., and Glockshuber, R. (1997) Quenching of tryptophan fluorescence by the active-site disulfide bridge in the DsbA protein from *Escherichia coli*. *Biochemistry 36*, 6391–6400.
34. Eyles, S. J., and Gierasch, L. M. (2000) Multiple roles of prolyl residues in structure and folding. *J. Mol. Biol. 301*, 737–747.
35. Steiner, R. F., and Kirby, E. P. (1969) The interaction of the ground and excited states of indole derivatives with electron scavengers. *J. Phys. Chem. 73*, 4130–4135.
36. Baskakov, I. V., and Bolen, D. W. (1998) Monitoring the sizes of denatured ensembles of staphylococcal nuclease proteins: Implications regarding m values, intermediates, and thermodynamics. *Biochemistry 37*, 18010–18017.

37. Becktel, W. J., and Schellman, J. A. (1987) Protein stability curves. *Biopolymers 26*, 1859–1877.
38. Uversky, V. (1993) Use of fast protein size-exclusion liquid chromatography to study the unfolding of proteins which denature through the molten globule. *Biochemistry 32*, 13288–13298.
39. Wilkins, D. K., Grimshaw, S. B., Receveur, V., Dobson, C. M., Jones, J. A., and Smith, L. J. (1999) Hydrodynamic radii of native and denatured proteins measured by pulse field gradient NMR techniques. *Biochemistry 38*, 16424–16431.
40. Damaschun, G., Damaschun, H., Gast, K., Gernat, C., and Zirwer, D. (1991) Acid denatured apo-cytochrome *c* is a random coil: Evidence from small-angle X-ray scattering and dynamic light scattering. *Biochim. Biophys. Acta 1078*, 289–295.
41. Geierhaas, C. D., Nickson, A. A., Lindorff-Larsen, K., Clarke, J., and Vendruscolo, M. (2007) BPPred: A Web-based computational tool for predicting biophysical parameters of proteins. *Protein Sci. 16*, 125–134.
42. Burchard, W., Schmidt, M., and Stockmayer, W. H. (1980) Information on polydispersity and branching from combined quasi-elastic and integrated scattering. *Macromolecules 13*, 1265–1272.
43. Flory, P. J. (1969) *Statistical mechanics of chain molecules*, Wiley, New York.
44. Kohn, J. E., Millett, I. S., Jacob, J., Zagrovic, B., Dillon, T. M., Cingel, N., Dothager, R. S., Seifert, S., Thiyagarajan, P., Sosnick, T. R., Hasan, M. Z., Pande, V. S., Ruczinski, I., Doniach, S., and Plaxco, K. W. (2004) Random-coil behavior and the dimensions of chemically unfolded proteins. *Proc. Natl. Acad. Sci. U.S.A. 101*, 12491–12496.
45. LeGuillou, J. C., and Zinn-Justin, J. (1977) Critical exponents for the n-vector model in three dimensions from field theory. *Phys. Rev. Lett. 39*, 95–98.
46. Schmid, F. X. (1989) Spectral methods of characterizing protein conformation and conformational changes, in *Protein Structure: A Practical Approach* (Creighton, T. E., Ed.) pp 251−285, IRL Press, Oxford.
47. Klitgaard, S., Neves-Petersen, M. T., and Petersen, S. B. (2006) Quenchers induce wavelength dependence on protein fluorescence lifetimes. *J. Fluoresc. 16*, 595–609.
48. Chen, J., Flaugh, S. L., Callis, P. R., and King, J. (2006) Mechanism of the highly efficient quenching of tryptophan fluorescence in human γ D-Crystallin. *Biochemistry 45*, 11552–11563.
49. Neves-Petersen, M. T., Gryczynski, Z., Lakowicz, J., Fojan, P., Pedersen, S., Petersen, E., and Petersen, S. B. (2002) High probability of disrupting a disulphide bridge mediated by an endogenous excited tryptophan residue. *Protein Sci. 11*, 588–600.
50. Bent, D. V., and Hayon, E. (1975) Excited state chemistry of aromatic amino acids and related peptides. III. Tryptophan. *J. Am. Chem. Soc. 97*, 2612–2619.
51. Gualfetti, P. J., Iwakura, M., Lee, J. C., Kihara, H., Bilsel, O., Zitzewitz, J. A., and Matthews, R. C. (1999) Apparent radii of the native, stable intermediates and unfolded conformers of the α-subunit of tryptophan synthase from *E. coli*, a TIM barrel protein. *Biochemistry 38*, 13367–13378.

BI800554V